

Four-wave mixing with time-delayed, correlated, phase-diffusing optical fields

Gautam Vemuri

*Department of Physics, Indiana University–Purdue University at Indianapolis, 402 North Blackford Street,
Indianapolis, Indiana 46202-3273*

(Received 17 March 1993)

Four-wave mixing in homogeneously broadened, two-level atoms, driven by time-delayed, correlated phase-diffusing optical fields is investigated. The spectrum of the driving field has an arbitrary bandwidth, i.e., it can have a Lorentzian or a Gaussian profile or an intermediate profile (Voigt). A time delay between the strong pump and weak probe field provides a partial correlation between the fields, and this time delay makes the composite field seen by the atoms non-Markovian. It is shown that the calculation of the four-wave-mixing signal reduces to the solution of six coupled Langevin equations with multiplicative noise; Monte Carlo techniques are utilized to study the response of the atoms to non-Markovian fields. A technique for numerically simulating phase-diffusing fields with colored frequency fluctuations is shown. The four-wave-mixing profiles are found to be significantly different from those for which the driving field is chaotic. The profiles show oscillatory behavior as evidence of the Rabi frequency, a feature not seen in previous works. For some parameter values, a revival of the signal is seen for an increasing time delay, analogous to the revivals seen in chaotic field signals [Phys. Rev. A **44**, 6009 (1991)].

PACS number(s): 42.50.Md, 42.65.Vh

I. INTRODUCTION

Recently, there has been considerable interest in the study of atoms interacting with fluctuating fields [1–5]. In particular, it has been recognized that atomic observables that depend on higher-than-second-order electric-field correlations are very sensitive to the nature of the pump fluctuations. Zoller and co-workers have studied the problem of fluctuations in fluorescence intensity from two-level atoms (an observable related to fourth-order field correlations) driven by phase-diffusing fields and phase-jump fields and shown the results to be sensitive to the field statistics [6]. Later, these workers extended their work to study fluctuations in fluorescence intensity when two-level atoms are driven by fields with correlated amplitude and phase fluctuations (as could arise in a diode laser) and showed the results to be sensitive to these correlations [7]. The predictions of [6] were experimentally verified by Anderson *et al.* [8]. Elliott and co-workers have carried out experiments on two-photon absorption in sodium vapor where the signal is again proportional to the fourth-order field correlations [9]. These experiments were carried out for phase-diffusing fields, real Gaussian fields and chaotic fields and the results were different for each case, indicating a behavior of the observable that was sensitive to field statistics. Recently, we have reported on Monte Carlo calculations to compare the behavior of four-wave mixing in two-level atoms driven by chaotic and phase-diffusing fields [10]. Camparo and Lambropoulos have also developed Monte Carlo methods to study atoms interacting with fields having correlated amplitude and phase fluctuations [11].

Of late, there has also been significant interest in atomic response to time-delayed correlated fields [12–15]. In these studies, an initial fluctuating field is split into two

or more parts, such that all fields have correlated fluctuations, and the beams are sent into an atomic medium. By time delaying one of these fields (by passing through an optical fiber, for example) with respect to the other(s), it is possible to have partial correlation between the fields and hence study atomic response to such time-delayed fields. In such studies, the atoms see the fluctuations (of amplitude or phase or both) on the first field and some time later see the same fluctuations on the second beam. By studying the signal as a function of the time delay, one can address the question, how well does the atom remember the fluctuations on the first beam?

In the context of atomic interactions with non-Markovian fields, four-wave mixing (FWM) is the commonly studied observable. One reason of course is that FWM, by its very nature, requires multiple beams, and hence offers the possibility of time delays between various beams. A strong motivation for focusing on four-wave mixing is that time-delayed four-wave mixing has been proposed as a practical technique for measuring fast dephasing phenomena in atomic media. Traditional methods for measuring these phenomena rely on ultrashort pulse lasers, which are expensive and restricted to a small-wavelength region of the spectrum. It was proposed by Morita and Yajima [16] that using time-delayed, correlated, incoherent fields can serve as an alternative scheme for measuring these fast phenomena. These authors established that the shortest dephasing times that can be measured with incoherent light are limited by the correlation time of the fluctuating field. Since it is much simpler to produce incoherent light with short correlation times than ultrashort pulses, this technique is indeed a powerful one. Morita and Yajima's work dealt with weak, chaotic, broadband fields, i.e., δ -function correlated fluctuations. Other related works in this con-

text include that of Agarwal [17] on weak, chaotic fields with finite bandwidths. Tchenio *et al.* [18] have used diagrammatic methods to calculate the signals due to time-delayed pulses. These authors also considered the case of inhomogeneous broadening of the atomic medium and assumed the correlation time of the pulses to be very short, thus allowing the use of the decorrelation approximation. They also reported experimental results on the response of two-level atoms to time-delayed pulses [19]. We have recently presented results for time-delayed four-wave mixing in chaotic fields of arbitrary bandwidths and pump intensities [20].

All previously mentioned works with non-Markovian fields have been in the context of chaotic fields. While four-wave mixing has been the commonly studied atomic observable, Gheri, Marte, and Zoller [21] have recently studied the problem of absorption by two-level atoms of a weak, time-delayed, phase-diffusing probe field in the presence of a strong, correlated pump field. The predictions of this work were verified by Anderson *et al.* [22]. In Ref. [21], an elegant propagation operator technique was developed to study atomic interactions with non-Markovian fields. This paper dealt with the pure phase-diffusing model, i.e., the frequency fluctuations were δ -function-correlated and the driving field spectrum was a Lorentzian. It is our understanding that extending these techniques to a phase-diffusing field with non- δ -function-correlated frequency fluctuations may not be straightforward, if not infeasible. This serves as an impetus for us to develop numerical techniques which can address phase-diffusing fields with colored frequency fluctuations. This paper reports results of four-wave mixing in two-level atoms where the non-Markovian fields obey a phase-diffusion model. As stated earlier, with the exception of the work in [22], all previous experiments on laser-atom interactions with non-Markovian fields have been with chaotic fields. One motivation for this paper is the experiments currently under way by Elliott and Smith [23] to study FWM in time-delayed, phase-diffusing optical fields. These experiments utilize a technique developed by Elliott and Smith to superimpose phase or frequency fluctuations on the output of a highly stabilized dye laser, using acousto-optic and electro-optic methods [24].

Some recent papers by Finkelstein and Berman have dealt with two-level atoms interacting with non-Markovian fields, where the pump field is strong [25]. In these works the authors consider the depletion of the ground state, but require that the bandwidth of the field be larger than the Rabi frequency of the pump. However, just as in [20], the Monte Carlo techniques allow us to relax this requirement and consider situations where the bandwidth of the field is smaller than the Rabi frequency of the pump and yet include depletion of the ground state by the strong pump (pump induced saturation effects are thus accounted for). The relaxation of this assumption is possible with the techniques of Gheri, Marte, and Zoller also [21].

In the following section we present the theoretical background for our work. We show that the calculation of the four-wave mixing signal reduces to the numerical solution of six coupled Langevin equations, with multipli-

cative noise. In the section after that we briefly discuss the properties of a phase-diffusing optical field and present a technique for numerically simulating such a field for arbitrary fluctuation parameters. In the last section we present our results on FWM in time-delayed fields for a wide range of parameter values.

II. FOUR-WAVE MIXING IN TWO-LEVEL ATOMS IN PHASE-DIFFUSING, NON-MARKOVIAN FIELDS

We represent the electric field interacting with the two-level atoms by

$$E(t) = \exp(-i\omega_1 t + i\mathbf{k}_1 \cdot \mathbf{r}) \hat{\mathbf{e}} \epsilon(t) + \exp(-i\omega_1 t + i\mathbf{k}_s \cdot \mathbf{r}) g \hat{\mathbf{e}} \epsilon(t - \tau). \quad (2.1)$$

The total field is thus the sum of two separate fields, the strong pump (subscript 1) and the weak, time-delayed probe (subscript s). ω_1 is the driving field frequency and is the same for both fields. \mathbf{k}_1 and \mathbf{k}_s are the wave vectors for the two fields and $\hat{\mathbf{e}}$ is the unit polarization vector. The time delay between the pump and the probe is accounted for by τ and can be varied as desired. The factor g accounts for the weak probe and in general $g \ll 1$.

The field described above, with a pump field in the direction \mathbf{k}_1 and a probe field in the direction \mathbf{k}_s , interacts with an ensemble of homogeneously broadened, two-level atoms. Both fields are derived from the same source and are time delayed with respect to each other. Further, since both fields are derived from the same source, they are at the same frequency. The degenerate FWM signal is generated in the direction $2\mathbf{k}_1 - \mathbf{k}_s$. We choose to model the electric field as a phase-diffusing field, where the amplitude of the field is a constant but the phase or frequency is a stochastic quantity. In several spectroscopic experiments, one uses a single-mode dye laser. These lasers, when operated far above threshold, as they typically are, mimic a phase-diffusing field quite accurately.

The dynamical behavior of two-level atoms interacting with a field described by (2.1) is governed by the optical Bloch equations. Let Ψ_1 , Ψ_2 , and Ψ_3 denote the components of the atomic dipole moments and population inversion, respectively. In this notation, we denote the density matrix operator by ρ , the off-diagonal elements of the density matrix, ρ_{12} and ρ_{21} , are given by Ψ_1 and Ψ_2 , and Ψ_3 equals $\frac{1}{2}(\rho_{11} - \rho_{22})$, i.e., one-half the difference in the population of the excited state and the ground state. On transforming to a frame rotating with the frequency of the driving field, ω_1 , the Bloch equations can be written as

$$\frac{d\tilde{\Psi}}{dt} = M\tilde{\Psi} + I, \quad (2.2)$$

where

$$M = \begin{bmatrix} -\frac{1}{T_2} + i\Delta & 0 & -2ix^*(t) \\ 0 & -\frac{1}{T_2} - i\Delta & 2ix(t) \\ -ix(t) & ix^*(t) & -\frac{1}{T_1} \end{bmatrix}. \quad (2.3)$$

Here Δ is the detuning parameter between the atomic frequency and the driving field frequency, i.e., $\Delta = \omega_0 - \omega_1$,

$$\begin{aligned} x(t) &= \frac{\mathbf{d} \cdot \hat{\boldsymbol{\epsilon}}}{\hbar} \{ \epsilon(t) + \exp[i(\mathbf{k}_s - \mathbf{k}_1) \cdot \mathbf{r}] g \epsilon(t - \tau) \}, \\ \tilde{\Psi}_1 &= \exp(-i\omega_1 t + i\mathbf{k}_1 \cdot \mathbf{r}) \Psi_1, \\ \tilde{\Psi}_3 &= \Psi_3, \\ I_1 &= I_2 = 0, \\ I_3 &= -\frac{1}{2T_1}, \end{aligned} \quad (2.4)$$

and we define $u = T_2/T_1$. In these equations T_1 and T_2 are the usual longitudinal and transverse relaxation times of the atomic system. In our work, all time units have been normalized to T_2 . Following the prescription in [20], we calculate the FWM signal (forward geometry) to all orders in the strong pump field and to first order in the weak probe field. We thus obtain

$$\tilde{\Psi} = \tilde{\Psi}^{(0)} + \tilde{\Psi}^{(1)} + \tilde{\Psi}^{(2)} + \dots, \quad (2.5)$$

where $\Psi^{(0)}$ and $\Psi^{(1)}$ are given by

$$\frac{d\tilde{\Psi}^{(0)}}{dt} = M^{(0)}\tilde{\Psi}^{(0)} + I \quad (2.6)$$

and

$$\frac{d\tilde{\Psi}^{(1)}}{dt} = M^{(0)}\tilde{\Psi}^{(1)} + M^{(1)}\tilde{\Psi}^{(0)}. \quad (2.7)$$

$M^{(0)}$ is obtained from (2.3) by setting $g = 0$, $M^{(1)}$ from (2.4) with $1/T_2 = \Delta = 1/T_1 = 0$, and

$$x(t) = \frac{\mathbf{d} \cdot \hat{\boldsymbol{\epsilon}}}{\hbar} g \epsilon(t - \tau) \exp[i(\mathbf{k}_s - \mathbf{k}_1) \cdot \mathbf{r}]. \quad (2.8)$$

Equation (2.7) is applicable for time evolution of the system when t is greater than or equal to τ , since the probe starts acting at time τ . We write the solution of (2.7) as

$$\tilde{\Psi}^{(1)} = \exp[i(\mathbf{k}_s - \mathbf{k}_1) \cdot \mathbf{r}] A + \exp[i(\mathbf{k}_s - \mathbf{k}_1) \cdot \mathbf{r}] F \quad (2.9)$$

and the column matrix is given by the solution of

$$\frac{dF}{dt} = M^{(0)}F + ig \frac{\mathbf{d} \cdot \hat{\boldsymbol{\epsilon}}}{\hbar} \epsilon^*(t - \tau) \begin{bmatrix} -2\tilde{\Psi}_3^{(0)}(t) \\ 0 \\ \tilde{\Psi}_2^{(0)}(t) \end{bmatrix}. \quad (2.10)$$

Equations (2.6) and (2.10) are the coupled Langevin equations with multiplicative noise that need to be solved. The FWM signal in homogeneously broadened media is proportional to S , given by

$$S = \lim_{t \rightarrow \infty} \langle F_2^*(t) F_2(t) \rangle. \quad (2.11)$$

In (2.11), the angular brackets denote stochastic averaging over the fluctuations of the field [to see the connection between (2.11) and calculation of four-wave mixing signals via the third-order nonlinear susceptibility, see [16,26]]. We numerically integrate (2.6) and (2.10) and,

using Monte Carlo methods, calculate S for a range of values of field parameters.

To explicitly incorporate the phase-diffusing optical fields, we define the quantity $x(t)$ as

$$x(t) = \Omega \exp[i\phi(t)], \quad (2.12)$$

where Ω is the Rabi frequency of the pump (taken to be real) and $\phi(t)$ is the time-dependent stochastic phase. Thus the stochastic frequency is given by

$$\mu(t) = \frac{d\phi(t)}{dt}, \quad (2.13)$$

where $\mu(t)$ represents the fluctuations in the driving field frequency about the frequency ω_1 . It is assumed to be a Gaussian, Markov process with zero mean and a second-order correlation function by

$$\langle \mu(t)\mu(t') \rangle = b\beta \exp(-\beta|t - t'|), \quad (2.14)$$

where b is the strength of the noise (or spectral density) and β is the bandwidth of the noise. The product $b\beta$ is the variance of the noise process. Since $\mu(t)$ is taken to be a Gaussian process, specifying its first two moments completely specifies the process. For values of $\beta \gg b$, (2.14) reduced to a δ -function-correlated process

$$\langle \mu(t)\mu(t') \rangle = 2b\delta(t - t'). \quad (2.15)$$

In this case, the field power spectrum has a Lorentzian profile with a full width at half maximum (FWHM) given by $2b$. In the other extreme, when $\beta \ll b$, the field spectrum is a Gaussian with a FWHM related to the product $b\beta$. For intermediate values of b and β , the field spectrum has a Voigt profile. Thus by varying the relative values of b and β , it is possible to study the effects of field line shapes on atomic response.

III. NUMERICAL SIMULATION OF PHASE-DIFFUSING FIELDS

In this section we discuss briefly some of the properties of a phase-diffusing field and the numerical simulation of these fields. Elliott and Smith have discussed the properties of such fields in detail, and reported on methods for producing these fields (with precisely controlled and defined statistics) in the laboratory [24]. We denote the stochastic phase by $\phi(t)$ and the stochastic frequency, which is the time derivative of $\phi(t)$, by $\mu(t)$. As stated in the previous section, $\mu(t)$ is assumed to be a Gaussian-Markov process and its properties completely defined by (2.14). In the event of the frequency fluctuations being δ -function correlated, the correlation function of $\mu(t)$ is given by (2.15).

In order to numerically simulate the frequency fluctuations, we take

$$\frac{d\phi}{dt} = F_\phi(t), \quad (3.1)$$

where $F_\phi(t)$ is a fluctuating quantity with the desired correlation function. On integrating this equation, we get

$$\phi(t + \Delta t) = \phi(t) + \int_t^{t+\Delta t} dt' F_\phi(t') \quad (3.2)$$

which can then be rewritten as

$$\phi(t + \Delta t) = \phi(t) + X_1(t), \quad (3.3)$$

where

$$X_1(t) = \int_t^{t+\Delta t} dt' F_\phi(t') \quad (3.4)$$

represents Gaussian random numbers with zero mean and the desired variance. If the correlation function of $F_\phi(t)$ is given by

$$\langle F_\phi(t) F_\phi(t') \rangle = 2b\delta(t - t'), \quad (3.5)$$

then $X_1(t)$ has variance of $2b\Delta t$, where Δt is the numerical integration step size. If the form of the correlation function is given by

$$\langle F_\phi(t) F_\phi(t') \rangle = b\beta \exp(-\beta|t - t'|), \quad (3.6)$$

then the variance of the random process is given by the product $b\beta$. Here β is the bandwidth of the fluctuations.

To generate the fluctuations with δ -function-correlations, we use the Box-Mueller algorithm and generate Gaussian distributed random numbers, g_w (subscript denotes white noise), with zero mean and a variance of $2b\Delta t$,

$$g_w = [-4b\Delta t \ln(\eta_1)]^{1/2} \cos(2\pi\eta_2), \quad (3.7)$$

where η_1 and η_2 are computer generated, uniformly distributed random numbers between 0 and 1. The phase is then given by

$$\phi(t + \Delta t) = \phi(t) + g_w. \quad (3.8)$$

If ϕ is larger than 2π , we subtract 2π from it and if ϕ is smaller than zero, we add 2π to it, to restrict ϕ to the physically meaningful $0-2\pi$ range. The associated field spectrum has a Lorentzian line shape with a FWHM of $2b$.

As stated earlier, the problem of atoms interacting with non-Markovian, phase-diffusing fields with colored frequency fluctuations is a very complicated one and perhaps can be solved only by numerical methods. In order to simulate such a phase-diffusing field (colored noise), we resort to a very accurate algorithm developed by Fox, *et al.* [27]. We state the outline of the method here and refer the reader to Refs. [27,28] for further details. The expression for the colored noise, $\epsilon_c(t)$ (subscript denotes colored noise), is given by

$$\epsilon_c(t + \Delta t) = \epsilon_c(t) \exp(-\beta\Delta t) + h, \quad (3.9)$$

where h is the source term producing the colored noise. h obeys Gaussian statistics, has a zero mean and a second moment given by

$$\langle h^2(t, \Delta t) \rangle = b\beta[1 - \exp(-2\beta\Delta t)]. \quad (3.10)$$

h is obtained from the Box-Mueller algorithm,

$$h = \{-2b\beta[1 - \exp(-2\beta\Delta t)] \ln(\eta_1)\}^{1/2} \cos(2\pi\eta_2). \quad (3.11)$$

The colored noise thus obtained from (3.9) has a zero

mean and a variance of $b\beta$. The time-dependent, fluctuating phase is then obtained from

$$\phi(t + \Delta t) = \phi(t) + \epsilon_c(t). \quad (3.12)$$

As before, it is necessary to ensure that ϕ lies in the $0-2\pi$ range. We have shown in [28] that for values of $\beta \gg b$, the associated field spectrum is a Lorentzian with a FWHM of $2b$, while for $\beta \ll b$, the field spectrum is a Gaussian with a FWHM related to $b\beta$. For values of β between these two extremes the field spectrum has a Gaussian peak and Lorentzian tails, i.e., the tails decay slower than for a Gaussian. We have also shown in [28] that the field spectra obtained from our simulations give excellent agreement with fitted Lorentzian and Gaussian profiles (with appropriate FWHM) as well as for the intermediate profiles.

We use the fluctuations simulated here, in (2.6) and (2.10), and solve the set of coupled Langevin equations numerically. An Euler method was used for the numerical integration, with a time step of $10^{-4}T_2$. In our preliminary runs, results obtained from the Euler integration method were compared with those obtained from a fourth-order Runge-Kutta method (RK). We tested the consistency of our numerical results for each of these two methods by progressively reducing the step size by half, until further reduction in step size did not effect the results. The final step size chosen was 10 times smaller than the step size where this condition was satisfied. It is normally expected that the RK method, while slower than the Euler method, allows one to use a larger integration step size to offset the loss of speed. Our calculations indicated that the RK method would work with a step size 5 times larger than the one we used for the Euler method. However, the results from the two methods were identical (within 1%) with the Euler method being substantially faster. We found that the accuracy of the results obtained with the Euler method, for the problem under study, was dependent on the step size and the number of trajectories over which the averaging was performed, and hence appropriate choices for these parameters were made. The set of equations (2.6) were first numerically integrated up to a time t where $0 \leq t \leq \tau$, with the initial conditions $\Psi_1(t=0) = \Psi_2(t=0) = 0$ and $\Psi_3(t=0) = -0.5$. The values of the electric field $x(t)$ were stored. After a time τ , (2.10) and (2.6) were simultaneously solved, with the stored values of $x(t)$ used in (2.10). This accounted for the delay between the pump and the probe. The initial conditions on (2.10) were $F_1(0) = F_2(0) = F_3(0) = 0$. The time delay τ was variable in our work and the FWM signal studied as a function of τ . For a given τ , the values of F_2 were allowed to reach a steady state and from these steady-state values the FWM signal was extracted as in (2.11). The signal in our work represents an averaging over at least 5000 trajectories, each with a different set of random numbers. This ensured that our results were not effected by small statistics. To test this, we performed five different averages over as many as 10000 trajectories, each with a completely different set of random numbers. This was done for the representative cases of $\beta=1$ and $b=10$, $\beta=100$ and

$b=1$, and $\beta=10$ and $b=10$ for an Ω of 6.0. In every case the results were within 3% of the results obtained with 5000 averages. The computed FWM signal was then plotted as a function of τ .

In order to compute the FWM signal for negative time delays, i.e., where the strong pump follows the weak probe in time, we modified (2.6) and (2.10) as follows: we replaced $x(t)$ by $x(t-\tau)$ for all $\tau \leq t \leq \infty$ in (2.6) and replaced $x^*(t-\tau)$ by $x^*(t)$ for all $0 \leq t \leq \infty$ in (2.10). The resulting equations were then solved exactly as for positive delays.

IV. RESULTS

In this section we report on the results for four-wave mixing profiles as a function of the time delay between a strong pump and a weak probe, when homogeneously broadened, two-level atoms interact with partially correlated fields. As stated earlier, the composite field seen by the atoms, due to the time delay between the pump and the probe fields, is a non-Markovian field. Our Monte Carlo methods are particularly useful and powerful for studying the effects of phase-diffusing fields with colored frequency fluctuations, where no analytical methods are available currently. All time units in our work are normalized to the transverse relaxation time of the atomic system, T_2 . Two independent parameters, b and β characterize the fluctuations properties of the field, and the FWM signal in this work is proportional to the strength of the weak probe, i.e., g^2 . Further, we have normalized all our signals to unity at zero delay (this was necessary to depict signals for several field parameter values on the same figure; as shown in [10], the signals can vary over several orders of magnitude with change in Ω for a given b and β).

In Fig. 1(a) we show results when $b=1$ and $\beta=100$. Since $\beta \gg b$, the field power spectrum is a Lorentzian with a FWHM of $2b$ ($=2$ in this case). The three curves shown are for varying Rabi frequencies, Ω , of the pump field of 1.0, $\sqrt{10}$, and 6.0. These values of the Rabi frequencies correspond to strong pumping of the two-level atomic system and the larger values of Ω lead to a strong depletion of the ground state. Further, since the bandwidth of the driving field is 2, values of Ω of $\sqrt{10}$ and 6.0 are cases where the Rabi frequency is larger than the field bandwidth. We find that there is a decay of the FWM signal with increasing delay between the pump and the probe (in these results, the pump leads the probe in time). For large delays, the signal settles to a steady-state value which is equal to the signal for two completely uncorrelated fields. We also note that for the strong-field situations, i.e., Ω of $\sqrt{10}$ and 6.0, there are regular oscillations in the FWM profile as the delay gets to larger values. These oscillations are at exactly the same frequency as the Rabi frequency, Ω (see, e.g., the profile for $\Omega=6.0$; since $\Omega/2\pi$ is almost 1, there should be 1 oscillation per atomic lifetime, T_1 , or 2 oscillations per T_2 , when $T_2/T_1=2$; see the arrows in the figure).

The origin of these oscillations can be understood in terms of a simple intuitive explanation underlying optical coherent transients and keeping in mind that the pump

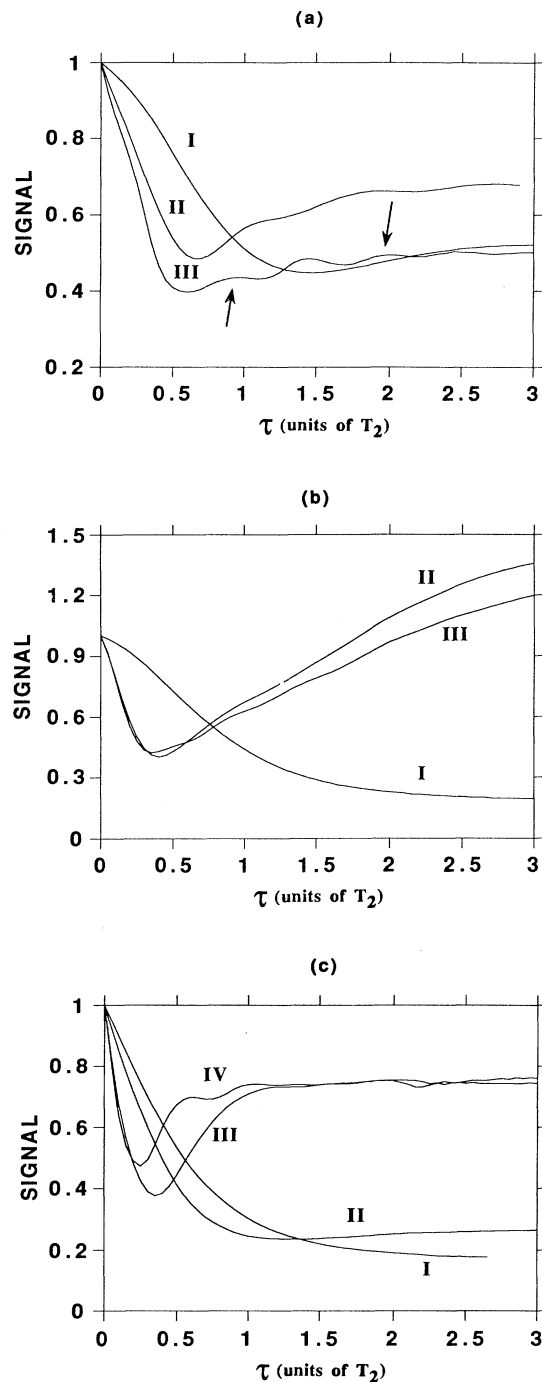


FIG. 1. (a) FWM signal as a function of time delay between pump and probe (in units of T_2) for $b=1$ and $\beta=100$ (Lorentzian field spectrum). The curves are for Rabi frequencies, Ω of 1.0 (I), $\sqrt{10}$ (II), and 6.0 (III). The arrows bracket two oscillations in a delay time of T_2 , as discussed in text. (b) FWM signal as a function of time delay between pump and probe (in units of T_2) for $b=10$ and $\beta=1$ (Gaussian field spectrum). The curves are for Rabi frequencies, Ω of 0.2 (I), $\sqrt{10}$ (II), and 6.0 (III). (c) FWM signal as a function of time delay between pump and probe (in units of T_2) for $b=10$ and $\beta=10$ (field spectrum intermediate to Gaussian and Lorentzian). The curves are for Rabi frequencies, Ω of 0.2 (I), 1.0 (II), $\sqrt{10}$ (III), and 6.0 (IV).

field is always on, i.e., we assume a continuous wave (cw) pump field. The fluctuations in the phase or frequency of the driving field induce transients in the coherence and the population difference between the two states of a two-level atom. These transients evolve at the Rabi frequency, Ω . For a monochromatic field, in the absence of any phase or frequency fluctuations, these transients would damp out on time scales related to the atomic relaxation times T_1, T_2 , and hence there would be no oscillations in the steady state. For fluctuating fields where Ω is less than either the atomic decay rate or the field bandwidth (i.e., weak-field regime), there are no oscillations in the coherence or the population difference associated with the two-level atoms. For strong-field situations, these oscillations are present and the field fluctuations continuously reinitiate the transients, thus sustaining the oscillations. This is where the assumption of a cw driving field is important, since a cw field provides a continuous train of fluctuations to trigger the transients. In other words, the atom is not undergoing free precession between correlated fluctuations of the pump and probe, but is being continuously driven by the fluctuating pump. The role of the fluctuations is thus to maintain the oscillations without their damping out and it is precisely these oscillations that show up in the FWM signal where the signal arises by scattering off the oscillating, transient grating (due to the oscillations in the coherence).

Previous works on FWM in time-delayed fields have not seen these oscillations, since they were restricted to chaotic fields [18–20,25]. In chaotic fields, the amplitude and hence the Rabi frequency itself is a stochastically fluctuating quantity. Hence, the oscillations on the FWM profiles as a function of the time delay get washed out by averaging over the fluctuating Ω . In case of the phase-diffusing fields, the value of Ω is a constant and shows up as oscillations on the FWM profiles. Such oscillations were also reported in [21]. For weak fields, say $\Omega=0.2$, there is a decay of the FWM signal as a function of the delay, τ (results not shown). No oscillations are seen on the profiles for weak fields since the Rabi frequency is smaller than the bandwidth of the driving field. We also note that the signal as a function of the delay decreases faster with increasing Rabi frequency. This is similar to the result for chaotic fields [20]. The background signals, i.e., the signals for large delays show a much different behavior for the two models; for chaotic fields, the signal at large delays for a given pump bandwidth, increases with increasing Rabi frequency, while no such regular behavior is seen for FWM signals in phase diffusing fields [10].

It is usually difficult to make a direct comparison of results obtained for phase-diffusing fields with those from chaotic fields. For phase-diffusing fields, the field line shapes can be Lorentzians or Gaussians, depending on the relative values of b and β . Further, the Rabi frequency is independent of the field parameters b and β . For chaotic fields, with a field correlation function as in [20], the field line shape is always a Lorentzian with a FWHM that depends only on the value of the bandwidth of the fluctuations. The Rabi frequency for chaotic fields is given by the square root of the product of the noise

strength and the noise bandwidth. In spite of these inherent incompatibilities, it is interesting to compare the results here with those from [20], which contains results on FWM in two-level atoms for time-delayed fields, where the fields are modeled as chaotic. We see that for phase-diffusing fields, when the bandwidth of the driving field is 2 and the Rabi frequency is $\sqrt{10}$, the signal decays with increasing time delay between the pump and the probe. The signal for uncorrelated fields, i.e., for large τ , is smaller than the signal for fully correlated fields, i.e., at $\tau=0$. However, for chaotic fields, with a bandwidth of 2 and Ω of $\sqrt{10}$, the signal for uncorrelated fields is larger than the signal for fully correlated fields (see Fig. 4 in [20]). In both cases, the fluctuations parameters are chosen such that the field line shapes are Lorentzians, and yet a dramatic difference in the FWM profiles is observed. This, of course, stems from the fact that FWM is a $\chi^{(3)}$ process, and the observable is thus related to the sixth-order electric-field functions. As pointed out by Zoller and co-workers [6,7], observables dependent on higher-order field correlations are very sensitive to the details of the driving field statistics, and hence we expect FWM to give different results for phase-diffusing field versus chaotic fields.

We next look at the other extreme of the field fluctuation parameters in Fig. 1(b), i.e., when $b=10$ and $\beta=1$. Here $\beta \ll b$ and hence the field spectrum is a Gaussian, with a FWHM related to the product $b\beta$. The linewidth in this case is equal to 3.7 approximately. The three curves are for $\Omega=0.2$ (weak fields), $\Omega=\sqrt{10}$, and $\Omega=6.0$. For weak fields, as expected we find a decay of the signal which finally settles for large delays to a value equal to that due to uncorrelated fields. However, for the strong-field situations, we find much different results. We note first of all that there are almost no oscillations on the profiles for $\Omega=\sqrt{10}$. Here, the Rabi frequency is smaller (almost comparable) than the bandwidth of the driving field and hence the bandwidth washes out any oscillations. For $\Omega=6.0$, we see a little more stronger evidence of the Rabi oscillations on the FWM profiles. Another feature is that the signal for large delays (uncorrelated fields) is larger than the FWM signal at zero delay between the pump and the probe for Ω of $\sqrt{10}$ and 6.0. Such revival of the FWM signal was also noticed for some parameter values of chaotic fields, where the driving field was strong. In particular, it was reported in [20] that the revival occurs for a field bandwidth of unity (i.e., equal to atomic width). However, similar revivals of the signal were also reported for other parameters values in [18–20,25]. Further, such revival of the signals was seen in the absorption spectrum as a function of time delay, reported in [21]. In that work, the absorption spectrum shows a revival even for δ -function-correlated frequency fluctuations. We conclude from these results that this revival of the signal is a very robust phenomena, seen for different observables of the atomic system.

While the results presented in Fig. 1(a) can be obtained using the techniques presented in [21], the Monte Carlo method is very useful for obtaining results presented in Figs. 1(b) and 1(c). The latter figure reports on FWM profiles when $b=10$ and $\beta=10$. Since b and β are com-

parable, the field line shape is intermediate between a Lorentzian and a Gaussian, and has a bandwidth of 11.8 approximately [24]. We report results for $\Omega=0.2, 1.0, \sqrt{10}$, and 6.0. Since the bandwidth of the driving field is larger than the pump Rabi frequencies, there is very little evidence of oscillations on these profiles, even for strong fields. Whatever little oscillations there are, damp out rapidly. In these results, the bandwidth is at most a factor of 2 or 3 larger than Ω . If the bandwidth were even larger, there would be absolutely no trace of any oscillations. We also notice that the FWM signals go to the value of the signal for uncorrelated fields quite rapidly for these fluctuations parameters (after about a lifetime). We see from these results that the numerical techniques provide a way for studying atomic response in non-Markovian fields, with no restrictions on the relative values of the field and atom parameters.

The results presented in this paper assume radiative decay of the excited state of the atom and hence take $u = T_1/T_2 = 2$. It is, however, fairly straightforward to incorporate other values of u . We have done simulations for both Lorentzian and Gaussian field spectra for values of u between 0 and 2. We find results very similar to those of [16,20] for different u values and hence do not report them here.

While it is possible to analytically solve several classes of problems in laser-atom interactions, it is so only under the assumptions of either of weak fields or large bandwidths (either of frequency or amplitude fluctuations). When the Rabi frequency becomes very large, the Rabi flopping time can sometimes become shorter than the field correlation time and bring in some different features. It is precisely this class of problems, with large Ω and colored frequency fluctuations, that are not amenable to analytical solutions. In the rest of this paper we will look at some of these cases. In Fig. 2 are FWM profiles as a function of the pump-probe delay for $\Omega=6$ and three different fluctuations parameters. Quite clearly, when the bandwidth of the field is comparable to Ω , we see little or no oscillations on the profiles, consistent with our expect-

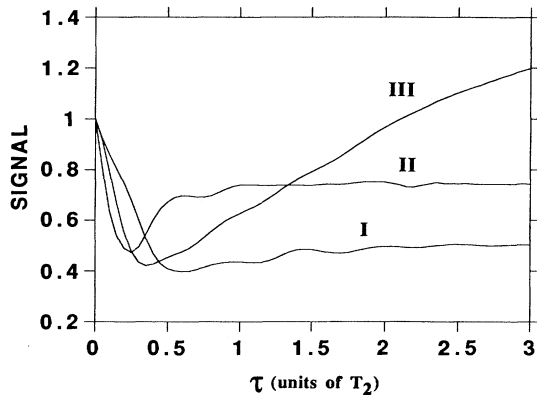


FIG. 2. FWM signal as a function of time delay between pump and probe (in units of T_2) for $\Omega=6.0$. The curves are for field parameters of $b=1, \beta=100$ (I); $b=10, \beta=10$ (II); and $b=10, \beta=1$ (III).

tations. If the bandwidth is larger than Ω , the oscillations get washed out. For the field bandwidth less than Ω , we do see prominent oscillations on the FWM profiles.

We have so far presented results only for positive delays, i.e., when the pump leads the probe in time. As shown in Sec. II, it is fairly easy to calculate the signals for negative delays as well, i.e., when the pump lags the probe in time. The results for both positive and negative delays are shown in Fig. 3(a) for $b=10, \beta=1$, and $\Omega=0.2$ (weak fields) and $\Omega=\sqrt{10}$ (strong fields). The qualitative behavior for negative delays is very similar to that of positive delays. The asymmetry in the uncorrelated signals for positive and negative delays is similar to those reported in [16,20] and can be partially attributed to the unequal strengths of the pump and probe fields. For weak fields there is a monotonic decay of the FWM signal while for strong fields we see a revival of the signal for large delays. The bandwidth here (3.7 approximately) is comparable to an Ω of $\sqrt{10}$ and hence we see little trace of oscillations on the signal even for strong fields. Finally in Fig. 3(b) we show results for a $b=10, \beta=10$,

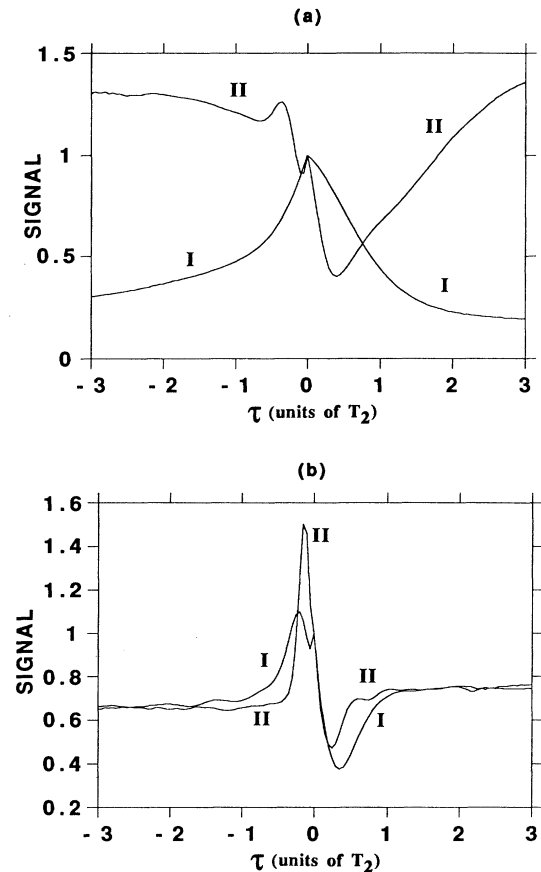


FIG. 3. (a) FWM signal as a function of positive and negative time delay between pump and probe (in units of T_2) for $b=10, \beta=1$ (Gaussian field spectrum), and $\Omega=0.2$ (I) and, $\Omega=\sqrt{10}$ (II). (b) FWM signal in strong fields as a function of positive and negative time delay between pump and probe (in units of T_2) for $b=10, \beta=10$, and $\Omega=\sqrt{10}$ (I) and $\Omega=6.0$ (II).

and Ω of $\sqrt{10}$ and 6.0. Here the bandwidth of the driving field is approximately 11.8 and hence larger than the Rabi frequencies. Hence, we expect no oscillations on our FWM signals. For Ω of 6.0, we see that for negative delays, the signal first increases and then decreases. This is qualitatively similar to the behavior seen in the absorption spectrum of [21], and can be explained in terms of an argument similar to the one in [22]. This figure deals with a situation where Ω is larger than $1/T_1$ but smaller than the field bandwidth. Due to the former condition, there is a depletion of the ground state during the time T_1 . However, due to the latter condition, the depletion is accumulated over several correlation times of the field. There is thus a diffusion of the Bloch vector during the time delay instead of a free precession, which leads to a degradation of the transient grating and hence reduction of the signal for large time delays.

In conclusion, we have studied the dependence of four-wave mixing signals in forward geometry, on the time delay between a strong pump and a weak, correlated probe. The pump and probe fields are assumed to obey the phase-diffusion model and we have enumerated a numerical technique for simulating such fields with arbitrary noise parameters. For strong pump fields, and when the Rabi frequency of the field exceeds the field bandwidth, we see oscillations on our FWM profiles. These oscillations are at the same frequency as the Rabi frequency. Such oscillations are not seen for amplitude fluctuating fields due to the averaging over such fluctuations. We also notice a sensitive dependence of the FWM profiles on the statistics of the driving field. The results for the phase-diffusing fields are significantly different from those obtained for a chaotic field [20], even when the two fields have the same bandwidth and line shapes. This is due to the fact that the field bandwidth depends only on the second-order field correlations and hence can be identical for the phase-diffusing and chaotic fields. However, the higher-order correlation functions are different for the

two models and if the observable depends on these higher-order correlations, the results can be quite different. Our FWM results in time-delayed fields thus complement those of previous workers who have demonstrated that observables that depend on higher than second-order field correlations are a sensitive indicator of the field statistics [6,7].

Finally, it should be mentioned that the model presented here might require a few modifications before a direct comparison with experiments can be made. We neglect Doppler broadening of the atomic medium completely in our analysis. It is, however, possible (and probable) that there might be some residual Doppler broadening, even for experiments in atomic beams. It is possible to modify our equations to incorporate such Doppler broadening. A more serious omission might be the finite length of the medium. Our work here assumes an infinitely thin medium. However, even in experiments in thin atomic beams, it is possible that one may have to account for the finite thickness of the atomic medium. However, we expect the techniques and results presented here to be a first step towards studying atomic interactions in non-Markovian, phase-diffusing optical fields of arbitrary field strengths, bandwidths, and band shapes.

ACKNOWLEDGMENTS

The author is pleased to acknowledge the interest of, and helpful discussions with Professor G. S. Agarwal, Professor J. Cooper, Professor D. S. Elliott, Professor S. J. Smith, Professor J. Cooper, Professor P. Zoller, and Dr. M. H. Anderson. He also thanks Professor D. S. Elliott for sharing information regarding their experiment. The computations were carried out on the VAX 8800 computer at IUPUI and help from Professor K. V. Vasavada and Professor F. T. Meiere is gratefully acknowledged.

-
- [1] See *Laser Noise*, edited by R. Roy [Proc. SPIE **1376** - 22 (1990)], and references therein.
 - [2] G. S. Agarwal, Phys. Rev. Lett. **37**, 1383 (1976); J. H. Eberly, *ibid.* **37**, 1387 (1976).
 - [3] G. Vemuri, R. Roy, and G. S. Agarwal, Phys. Rev. A **41**, 2749 (1990); G. Vemuri and G. S. Agarwal, *ibid.* **42**, 1687 (1990).
 - [4] R.E. Ryan and T. H. Bergeman, Phys. Rev. A **43**, 6142 (1991).
 - [5] A.G. Kofman, R. Zaibel, A. M. Levine, and Y. Prior, Phys. Rev. Lett. **61**, 251 (1988).
 - [6] The Halswanger, H. Ritsch, J. Cooper, and P. Zoller, Phys. Rev. A **38**, 5652 (1988).
 - [7] H. Ritsch, P. Zoller, and J. Cooper, Phys. Rev. A **41**, 2653 (1990).
 - [8] M. H. Anderson, R. D. Jones, J. Cooper, S. J. Smith, D. S. Elliott, H. Ritsch, and P. Zoller, Phys. Rev. Lett. **64**, 1346 (1990).
 - [9] D. S. Elliott, M. W. Hamilton, K. E. Arnett, and S. J. Smith, Phys. Rev. Lett. **53**, 439 (1984); Ce Chen, D. S. Elliott, and M. W. Hamilton, *ibid.* **68**, 3531 (1992); D. S. Elliott (private communication).
 - [10] G. S. Agarwal, G. Vemuri, C. V. Kanasz, and J. Cooper, Phys. Rev. A **46**, 5879 (1992).
 - [11] J. C. Camparo and P. Lambropoulos, Opt. Commun. **85**, 213 (1991).
 - [12] See, e.g., the special issue of J. Opt. Soc. Am. B **3** (1986), devoted to optical coherent transients.
 - [13] K. Kurokawa, T. Hattori, and T. Kobayashi, Phys. Rev. A **36**, 1298 (1987); K. Misawa, T. Hattori, and T. Kobayashi, Opt. Lett. **14**, 453 (1989).
 - [14] R. Beach, D. DeBeer, and S. R. Hartmann, Phys. Rev. A **32**, 3467 (1985).
 - [15] J. E. Golub and T. W. Mossberg, J. Opt. Soc. Am. B **3**, 554 (1986).
 - [16] N. Morita and T. Yajima, Phys. Rev. A **30**, 2525 (1984).
 - [17] G. S. Agarwal, Phys. Rev. A **37**, 4741 (1988).
 - [18] P. Tchenio, A. DeBarre, J. C. Keller, and J. L. LeGouet, Phys. Rev. A **39**, 1970 (1989); J. Opt. Soc. Am. B **5**, 1293 (1988); Phys. Rev. A **38**, 5235 (1988).
 - [19] P. Tchenio, A. DeBarre, J. C. Keller, and J. L. LeGouet, Phys. Rev. Lett. **62**, 415 (1989).

- [20] G. Vemuri, G. S. Agarwal, R. Roy, M. H. Anderson, J. Cooper, and S. J. Smith, *Phys. Rev. A* **44**, 6009 (1991).
- [21] K. Gheri, M. A. M. Marte, and P. Zoller, *J. Opt. Soc. Am. B* **8**, 1559 (1991).
- [22] M. H. Anderson, G. Vemuri, J. Cooper, P. Zoller, and S. J. Smith, *Phys. Rev. A* **47**, 3202 (1993).
- [23] D. S. Elliott and S. J. Smith (private communication).
- [24] D. S. Elliott and S. J. Smith, *J. Opt. Soc. Am. B* **5**, 1927 (1988).
- [25] V. Finkelstein and P. R. Berman, *Phys. Rev. A* **41**, 6193 (1990); **42**, 3145 (1990); *Proc. SPIE* **1376 - 22**, 68 (1991).
- [26] R. W. Boyd, *Nonlinear Optics* (Academic, San Diego, 1992).
- [27] R. F. Fox, I. R. Gatland, R. Roy, and G. Vemuri, *Phys. Rev. A* **38**, 5938 (1988).
- [28] G. Vemuri and R. Roy, *Opt. Commun.* **77**, 318 (1990).